10567
NACA TN 4227
TECH LIBRARY KAFB, NM
0066852

NATIONAL ADVISORY COMMITTEE FOR AERONAUTICS

TECHNICAL NOTE 4227

DRAG MINIMIZATION FOR WINGS IN SUPERSONIC FLOW, WITH VARIOUS CONSTRAINTS

By Max. A. Heaslet and Franklyn B. Fuller

Ames Aeronautical Laboratory
Moffett Field, Calif.

Washington
February 1958

AFMDC
L LIBRARY
AFL 2811

.E

TECH LIBRARY KAFB, NM

0066852

NATIONAL ADVISORY COMMITTEE FOR AERONAUTICS

TECHNICAL NOTE 4227

DRAG MINIMIZATION FOR WINGS IN SUPERSONIC FLOW, WITH VARIOUS CONSTRAINTS

By Max. A. Heaslet and Franklyn B. Fuller

SUMMARY

The minimization of inviscid fluid drag is studied for thin aerodynamic shapes subject to imposed constraints on lift, pitching moment, base area, or volume. The problem is transformed to one of determining a two-dimensional potential flow satisfying either Laplace's or Poisson's equations with boundary values fixed by the imposed conditions. By means of Kelvin's minimum energy theorem for harmonic fields, a method is given for approximate drag minimization in the case of given lift. For supersonic-edged wings with straight trailing edges, perfect analogies are established between cases involving lifting and nonlifting shapes. Particularly simple results are derived for a family of wings with curved leading edges with lift specified and center of pressure fixed at the 60-percent-chord position. General relations involving span load distribution and integrated loading along oblique cutting lines are derived. The minimum drag for other plan forms is determined and, in the case of nonlifting wings, difficulties associated with unreal shapes are discussed.

INTRODUCTION

The calculation of supersonic drag of wings or bodies and the reduction of the minimization problem to one of determining a harmonic function of the lateral coordinates was reported by Nikolsky in reference 1. Details of this method were not given, but a procedure leading to the same end that makes use of control surfaces which are everywhere inclined at the Mach angle to the streamwise direction was given by Ward in reference 2. Further work on the subject can be found in references 3 through 6. The drag is expressed by a surface integral over a surface that envelops upstream-facing Mach cones springing from the trailing edge of the wing or body. Drag minimization can then be re-expressed as a conventional isoperimetric problem once the desired constraints, such as, lift, pitching moment, base area, or volume, are represented in terms of integrals over the same control surface. Various forms of these representations have been given previously; for convenience they are given again here in uniform notation.

The several possible variational problems are set up in the form of partial differential equations (Laplace's or Poisson's) in terms of the lateral variables. The region in which the solution is to hold is determined by the original wing (or body), and the boundary conditions to be applied are determined by the constraints of the particular problem treated. Thus, although the problem has been reduced by one dimension, solution is usually not easy because the shape of the regions in which Laplace's equation is to be solved is not generally suited to mapping techniques, and the regions are, moreover, not simply connected. Numerical and approximate methods still apply, however, and particular families of solutions are readily found.

An approximate method for the problem of minimum drag with given lift is developed, based on Kelvin's principle of minimum energy of potential flows. The results involve the apparent area (or mass) of the boundaries, so in reality require knowledge of potential flows about such shapes. In practice, the procedure offers a means for rational approximation by enabling one to substitute known solutions for apparent area for the unknown ones of the problem at hand, and some examples are given.

In any control-surface method of calculation of integrated forces, etc., a certain amount of detailed information is lost. Thus, in the present case, local surface shape is not an element of the problem, except insofar as it influences, say, the base area or the volume. Therefore it is not, strictly speaking, possible to give assurance that a real wing can achieve the minimum drag given by a solution to the variational problem. This can happen when the conditions of the problem allow a solution that results in a crossing of the stream surfaces that form the wing. An example of the occurrence of this is given; namely, the yawed elliptic wing of given volume, with zero base area.

When the variational problems with the various constraints are listed, there is noted a similarity between the problems for given base area and for given lift, and those for given volume and for given pitching moment. Conditions under which the constraints are interchangeable in each of these two cases can be found; the result being that, for certain wings with supersonic edges, base area can be replaced by lift (or volume by pitching moment) without altering the drag of the wing. Such analog results have also been noted between optimum slender bodies and optimum lifting lines in subsonic flow.

A particularly simple solution can be determined exactly for one family of plan forms. This family has straight trailing edges and supersonic-type leading edges that are formed by sections of a hyperbola asymptotic to Mach lines. The constraints specify lift and center of pressure (or pitching moment). This family has two interesting limiting cases; at one extreme it becomes a sonic-edged triangle, and at the other a two-dimensional case. The triangular wing with sonic edges has been treated by Germain (ref. 4) and, by means of an approximation procedure, in reference 6, and comparisons with these results can be made. The span load distribution of these optimum wings is found directly from information

derived in the analysis. It is also possible to determine, less directly, additional knowledge of aerodynamic loading integrated along oblique lines. So long as the obliquity of the lines is such that the component of stream velocity normal to them is supersonic, the variation of the integrated loading in the stream direction is obtainable. The so-called chord load distribution is a special case of these results.

IMPORTANT SYMBOLS

A	base area of a wing or body
C_D	drag coefficient
C_L	lift coefficient
C_1,C_2	curves bounding a region in an x = const. plane (see sketch (b))
D	drag of a wing or body in a supersonic flow
$f(y,z)$	characteristic surface springing from a trailing edge (defined by $x = f(y,z)$)
h	deviation of body from control surface at trailing edge
l	streamwise extent of wing or body
L	lift
$\frac{L(x_0,\theta)}{q_\infty}$	integral of local loading $\left(\frac{\Delta p}{q_\infty}\right)$ along oblique line
m	tangent of the angle of sweep or yaw
M_∞	Mach number in the free stream
$\mathbb{M}$	pitching moment, positive for a nose-up moment, taken about the line $x = x_0$, $y = z = 0$
n	inner normal to a plane curve
N	inner normal to a surface
p	pressure
$\frac{\Delta p}{q_\infty}$	load coefficient (upper-surface pressure minus lower-surface pressure divided by free-stream dynamic pressure)

q_∞	free-stream dynamic pressure, $\frac{1}{2}\rho_\infty U_\infty^2$
s	arc length
S	region in an x = const. plane
x,y,z	Cartesian coordinates
x_o	x intercept of cutting line (see eq. (40))
U_∞	speed of free stream, parallel to x axis
V	volume of a wing or body
β^2	M_∞^2-1
Γ_1	space curve (defined in sketch (a))
λ,μ,σ,τ	Lagrange multipliers (see eq. (10))
μ_o	angle between oblique line and y axis (see eq. (40))
ρ	density
Σ_1,Σ_2	characteristic surfaces (see sketch (a))
φ	velocity potential
χ	perturbation potential on surface $x = f(y,z)$ (see eq. (2))
∇^2	two-dimensional Laplace operator, $\frac{\partial^2}{\partial y^2} + \frac{\partial^2}{\partial z^2}$

ANALYSIS

Expressions for the Drag and for Various Constraints

Consistent with linearized supersonic theory, the boundary conditions over a wing or body are specified on a cylindrical control surface with elements parallel to the stream direction. The positive x axis is alined with the free-stream direction, and the perturbation velocity components u,v,w induced by the wing or body in the x,y,z directions are given by the gradients of the perturbation velocity potential $\varphi(x,y,z)$ that is, by φ_x, φ_y, φ_z. The differential equation governing the flow field is

$$\beta^2\varphi_{xx}-\varphi_{yy}-\varphi_{zz} = 0 \tag{1}$$

where $\beta^2 = M_\infty{}^2-1$. The symbol M_∞ denotes free-stream Mach number and, in general, the subscript ∞ will be used to denote free-stream conditions, for example, U_∞ and ρ_∞ are free-stream velocity and density. As shown in sketch (a), the vertices of the downstream facing Mach cones trace out the leading edge of the control surface Σ_0 and the vertices of upstream facing Mach cones trace out its trailing edge. The surface Σ_0 is in this way enclosed by the envelopes Σ_1 and Σ_2 of two families of cones. The surfaces Σ_1 and Σ_2 intersect along the space curve Γ_1. As shown in sketch (b), the projection of Γ_1 in a plane $x = \text{const.}$ is the curve C_1. Similarly the control surface Σ_0 projects onto the curve C_2, and the surface Σ_2 projects onto the two-dimensional region S.

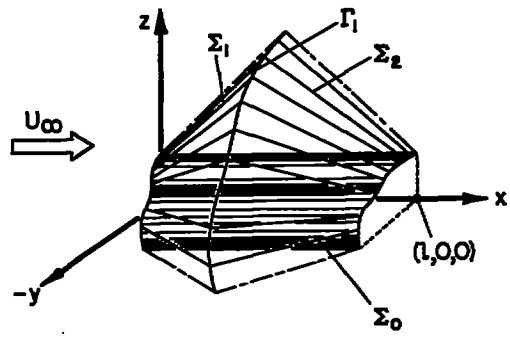

Sketch (a)

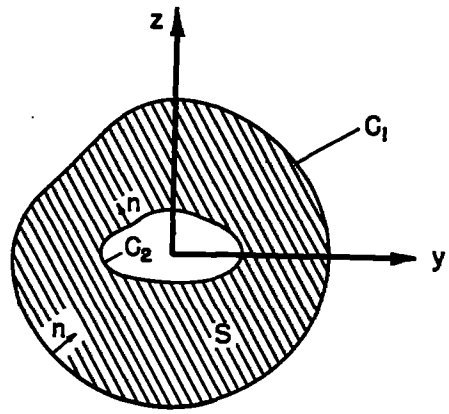

Sketch (b)

Let the surface Σ_2 be given by $x = f(y,z)$ and the value of the perturbation potential on Σ_2 be denoted by $\chi(y,z)$, that is,

$$\chi(y,z) = \varphi[f(y,z),y,z] \tag{2}$$

Wave drag D (plus vortex drag when lift occurs) is then given by the expression (ref. 2)

$$D = -\frac{\rho_\infty}{2}\iint_{\Sigma_2}(\chi_y{}^2+\chi_z{}^2)\cos(x,N)d\Sigma \tag{3a}$$

$$= -\frac{\rho_\infty}{2}\iint_S \chi\nabla^2\chi\, dy\, dz - \frac{\rho_\infty}{2}\int_{C_2}\chi\frac{\partial\chi}{\partial n}\, ds \tag{3b}$$

where $\cos(x,N)$ is the direction cosine relative to the x axis of the inner normal N to the surface Σ_2, ∇^2 is the two-dimensional Laplacian operator $(\partial^2/\partial y^2) + (\partial^2/\partial z^2)$ and $\partial\chi/\partial n$ is the gradient of the function χ along the inner normal to a curve in the yz plane.

In the succeeding paragraphs, formulae for base area, volume, lift, and pitching moment will be given. These results are applicable to any case in which the object of interest deviates only slightly from a cylindrical control surface. In reference 3, applications involving both planar surfaces and quasi-cylindrical bodies of revolution were given, but in this report the examples will include planar cases exclusively.

Consider a wing or body having thickness but without camber. If the thickness is zero at the leading edge, and the projection on a plane $x = \text{const.}$ of the deviation in area between the nose and tail of the body is A, it was shown in reference 3 that this area is given by

$$A = \frac{1}{U_\infty} \iint_{\Sigma_2} (\chi_y f_y + \chi_z f_z) \cos(x,N) d\Sigma \tag{4a}$$

$$= \frac{1}{U_\infty} \iint_S \chi \nabla^2 f \, dy \, dz + \frac{1}{U_\infty} \int_{C_2} \chi \frac{\partial f}{\partial n} ds \tag{4b}$$

$$= \frac{1}{U_\infty} \iint_S f \nabla^2 \chi \, dy \, dz + \frac{1}{U_\infty} \int_{C_1+C_2} f \frac{\partial \chi}{\partial n} ds \tag{4c}$$

When the aerodynamic shape is a wing, the curve C_2 is a segment of the y axis.

In reference 3 the volume enclosed by a nonlifting wing or body was expressed in the form

$$V = \int_{C_2} fh(f,s) ds - \frac{1}{2U_\infty} \iint_S \chi(2\beta^2 + \nabla^2 f^2) dy \, dz - \frac{1}{2U_\infty} \int_{C_2} \chi \frac{\partial f^2}{\partial n} ds \tag{5}$$

where $h(f,s)$ is the deviation from the control surface at the trailing edge. Equation (5) thus gives the volume of aerodynamic shapes that are either open or closed at the base. In two general cases, however, the first integral on the right in equation (5) can be deleted: first, when the wing or body closes, that is, when $h(f,s) = 0$; second, when the trailing edge is normal to the stream direction, and the origin of coordinates is either on the trailing edge, or the base area is zero, that is, either $f = 0$ or $\int_{C_2} h(f,s) ds = 0$. In these cases the volume formula is

$$V = -\frac{1}{2U_\infty}\iint_S \chi(2\beta^2+\nabla^2 f^2)\,dy\,dz - \frac{1}{2U_\infty}\int_{C_2}\chi\frac{\partial f^2}{\partial n}\,ds \tag{6a}$$

$$= -\frac{1}{2U_\infty}\iint_S f^2\nabla^2\chi\,dy\,dz - \frac{\beta^2}{U_\infty}\iint_S \chi\,dy\,dz - \frac{1}{2U_\infty}\int_{C_1+C_2} f^2\frac{\partial\chi}{\partial n}\,ds \tag{6b}$$

The base area or volume cannot be affected by the fore and aft placement of the origin used in the analysis; proper positioning can, however, sometimes be used to economize in algebraic manipulation.

Consider next a wing or body of zero thickness and carrying a load distribution by virtue of its camber and angle of attack. The lift L and pitching moment $\mathbb{M}$ about the line $x = x_m$, $z = 0$ can be expressed in terms of integrals over the control surface Σ_2 (see sketch (a)) in a manner directly analogous to that used for the evaluation of base area and volume. The lift formula (ref. 2) follows from the application of linearized theory to the force relation

$$\vec{F} = -\iint_{\Sigma_1+\Sigma_2} p\,\vec{N}\,d\Sigma - \iint_{\Sigma_1+\Sigma_2}\rho\,\vec{q}\,(\vec{q}\cdot\vec{N})\,d\Sigma$$

where

$\vec{F}$ vectorial force on configuration

$\vec{q}$ local velocity vector

$\vec{N}$ unit inner normal to Σ

p local pressure

ρ local density

The desired expression is

$$L = -\rho_\infty U_\infty \iint_S \chi_z\,dy\,dz \tag{7a}$$

$$= \rho_\infty U_\infty \int_{C_2}\chi\cos(z,n)\,ds \tag{7b}$$

The general moment integral is

$$\vec{\mathbb{M}} = \iint_{\Sigma_1+\Sigma_2} \rho(\vec{q}\cdot\vec{N})(\vec{r}_m \times \vec{q})d\Sigma + \iint_{\Sigma_1+\Sigma_2} p(\vec{r}_m \times \vec{N})d\Sigma$$

where $\vec{r}_m$ is the vector distance between the moment center and an integration element on the control surface. When $\mathbb{M}$ is positive for a nose-up pitching moment, linearized theory yields

$$\mathbb{M} = \rho_\infty U_\infty \iint_S \chi\, \nabla^2(zf)dy\, dz + \rho_\infty U_\infty \int_{C_2} \chi\left[\frac{\partial(zf)}{\partial n} - x_m\cos(z,n)\right]ds \tag{8}$$

When lift L is zero, or the pitching moment is calculated about the origin, one gets

$$\mathbb{M} = \rho_\infty U_\infty \iint_S \chi\, \nabla^2(zf)dy\, dz + \rho_\infty U_\infty \int_{C_2} \chi\, \frac{\partial(zf)}{\partial n}\, ds \tag{9a}$$

$$= \rho_\infty U_\infty \iint_S zf\, \nabla^2\chi\, dy\, dz + \rho_\infty U_\infty \int_{C_1+C_2} zf\, \frac{\partial\chi}{\partial n}\, ds \tag{9b}$$

Solutions of Variational Problems

The problem of minimizing drag under the constraint of given base area, or volume, or lift, or pitching moment can be set up with the aid of equations (3), (4), (6), (7), and (9). It is only necessary to apply standard variational methods to any one of the expressions

$$\left.\begin{aligned} I_1 &= D-\lambda A \\ I_2 &= D+\mu V \\ I_3 &= D-\sigma L \\ I_4 &= D-\tau\mathbb{M} \end{aligned}\right\} \tag{10}$$

where λ,μ,σ,τ are Lagrange multipliers. The sign of μ is taken differently so that all quantities λ,μ,σ,τ can be identified as characteristic parameters in the so-called combined flow field. Thus, μ is identified with pressure gradient in the combined field, a negative quantity. Any of these problems can be combined with another. For example, if it be required to find minimum drag with given base area and lift, the quantity to be minimized would be $D-\lambda A-\sigma L$ and so forth. The results found by applying the variational procedure to the expressions (10) will be given next. Each is a two-dimensional potential-flow problem in the lateral variables y,z.

Given base area:

$$\left.\begin{aligned} \nabla^2\left(\chi + \frac{\lambda}{\rho_\infty U_\infty} f\right) &= 0 \quad \text{in } S \\ \frac{\partial}{\partial n}\left(\chi + \frac{\lambda}{\rho_\infty U_\infty} f\right) &= 0 \quad \text{on } C_2 \\ \chi &= 0 \quad \text{on } C_1 \end{aligned}\right\} \tag{11a}$$

$$D = \frac{\lambda}{2} A \tag{11b}$$

Given volume (zero base area):

$$\left.\begin{aligned} \nabla^2\left(\chi + \frac{\mu}{2\rho_\infty U_\infty} f^2\right) &= -\beta^2 \frac{\mu}{\rho_\infty U_\infty} \quad \text{in } S \\ \frac{\partial}{\partial n}\left(\chi + \frac{\mu}{2\rho_\infty U_\infty} f^2\right) &= 0 \quad \text{on } C_2 \\ \chi &= 0 \quad \text{on } C_1 \end{aligned}\right\} \tag{12a}$$

$$D = -\frac{\mu}{2} V \tag{12b}$$

Given lift:

$$\left.\begin{aligned} \nabla^2\chi &= 0 \quad \text{in } S \\ \frac{\partial}{\partial n}\left(\chi + U_\infty \sigma z\right) &= 0 \quad \text{on } C_2 \\ \chi &= 0 \quad \text{on } C_1 \end{aligned}\right\} \tag{13a}$$

$$D = \frac{\sigma}{2} L \tag{13b}$$

Given pitching moment (zero lift, or moment center at origin):

$$\left.\begin{aligned} \nabla^2(\chi + U_\infty \tau z f) &= 0 \quad \text{in } S \\ \frac{\partial}{\partial n}(\chi + U_\infty \tau z f) &= 0 \quad \text{on } C_2 \\ \chi &= 0 \quad \text{on } C_1 \end{aligned}\right\} \tag{14a}$$

$$D = \frac{\tau}{2} \mathbb{M} \tag{14b}$$

In each of the problems listed as equations (11) through (14), the possibility of obtaining a solution depends primarily on the boundary curve C_1. Several cases where exact results could be obtained were discussed in reference 3. However, recourse to approximate methods is usually indicated. One such approximation, in which the wing is distorted by small amounts in order to achieve a solvable boundary curve C_1, is discussed in reference 6. Germain, reference 4, has used development in series. Another method, for the particular case of finding minimum drag at given lift, is discussed in the next section.

An Approximation of Minimum Drag Due to Lift by Energy Theorems

From equations (3), (7), and (13b), minimum drag for given lift takes the form

$$\begin{aligned} D &= \frac{1}{2} \rho_\infty \iint_S (\chi_y^2 + \chi_z^2)\,dy\,dz = -\frac{1}{2} \rho_\infty \int_{C_2} \chi \frac{\partial \chi}{\partial n}\,ds \\ &= \frac{\rho_\infty U_\infty \sigma}{2} \int_{C_2} \chi \cos(z,n)\,ds = \frac{\sigma}{2} L \end{aligned} \tag{15}$$

The first integral can be interpreted as the kinetic energy of a two-dimensional, incompressible fluid field (ρ_∞ = density) occupying the region S. Since the flow field is also irrotational, one is therefore

prompted to use classical methods of approximation to estimate the drag. Lord Kelvin's minimum theorem provides one such approach. It is stated by Lamb (ref. 7, p. 57) as follows:

> The irrotational motion of a liquid in a multiply-connected region has less kinetic energy than any other motion consistent with the same normal motion of the boundary and the same value of the total flux through each of the several independent channels of the region.

Consider, as in sketch (c), the minimum drag problem that arises when the wing trace lies well within the curve C_1. The potential field $\chi(y,z)$ will be assumed laterally symmetric. The boundary condition along the wing trace calls for a constant value of downwash. On the exterior curve C_1 the potential χ is a constant so that the stream lines of the disturbance field are normal to C_1. When C_1 is far distant from the wing trace, the flow field corresponds to the case of a two-dimensional flat plate moving downward in a fluid field of infinite extent. When C_1 is at a finite distance, an additional condition is imposed and, as a first approximation to the effect, one might assume that the flow in the vicinity of the plate is similar to the flow near a plate moving downward, at a different and slightly increased velocity in an unrestrained field. The magnitude of the difference in velocities must be determined by the boundary condition on C_1.

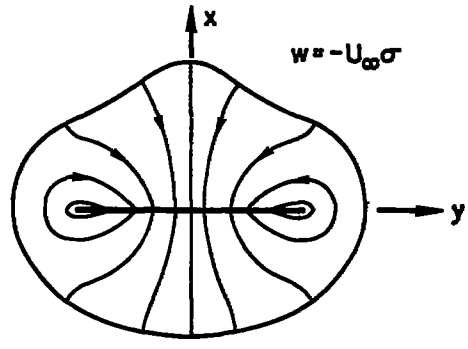

Sketch (c)

In order to use Kelvin's theorem it is convenient to start with the flow about the plate moving downward at a velocity of magnitude, say, $\sigma U_\infty - k$. Sketch (d) indicates the stream lines and the curve C_1 is shown dashed. The perturbation potential is

$$\Phi_1(y,z) = -(\sigma U_\infty - k)\varphi_1(y,z)$$

where $\varphi_1(y,z)$ is the perturbation potential for unit translational velocity. So long as the conditions in the flow are unchanged along the plate and at infinity, the kinetic energy of this irrotational field is a minimum. Consider, now, the following three potential fields:

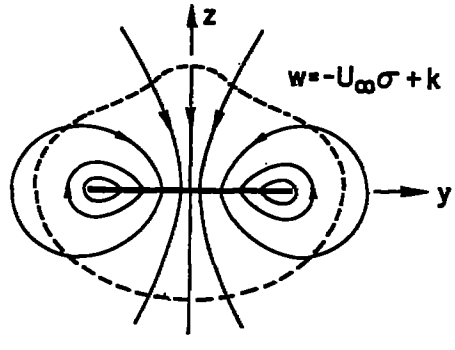

Sketch (d)

(a) The one in sketch (c) with $\chi(y,z)$ satisfying equations (13a). Set $\chi = -\sigma U_\infty \varphi$.

(b) A flow with uniform vertical velocity k within the boundary C_1. Its perturbation potential is $\Phi_2 = kz$.

(c) The flow associated with a downward velocity $-k'$ of the boundary C_1. Its perturbation potential is $\Phi_3 = -k'\varphi_3$, where φ_3 corresponds to unit translational velocity.

The sum of these three fields, see sketch (e), can be generated by imposing constraints along C_1 in the field of sketch (d) so long as k'

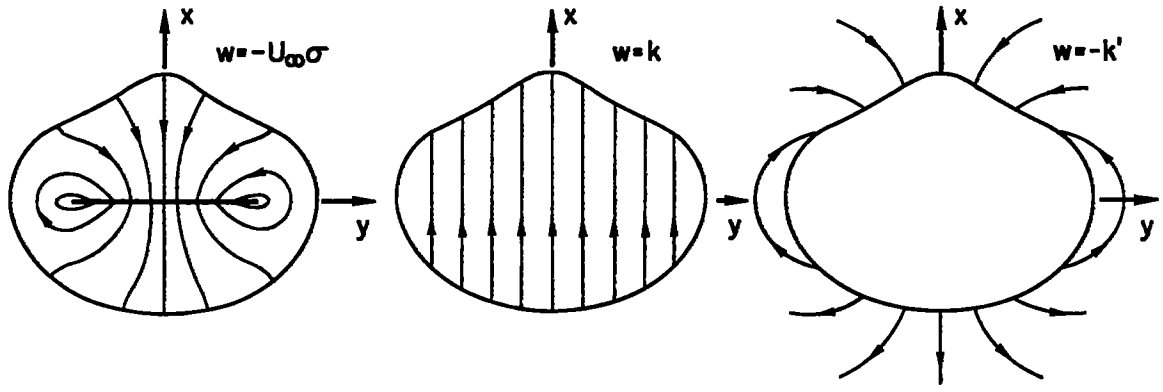

Sketch (e)

is chosen consistent with the flow conditions at infinity. In order to meet this demand one uses the fact that, far distant, the induced field of a solid in pure translation behaves as a doublet (ref. 7, p. 165). When the body is laterally symmetric, the axis of the doublet coincides with the axis of translation and the doublet or field strength is proportional to $A+Q$ where A is the additional apparent area of the body and Q its geometric area. For Φ_1 and Φ_3 to behave alike, therefore, the relation

$$(\sigma U_\infty - k)A_{W,\infty} = k'(A_{B,\infty}+Q) \tag{16}$$

must hold, where

$A_{W,\infty}$ apparent area of wing or plate in an infinite region

$A_{B,\infty}$ apparent area of the boundary C_1 in rigid vertical motion

Equation (16) thus establishes one linear relation between k and k', and it remains to establish one more.

In the original field of sketch (d) no discontinuity in normal or tangential velocity occurs along C_1 whereas the combined field of sketch (e) has discontinuities in both quantities. These discontinuities are a measure of the added constraints imposed on the original field.

Suppose, now, that k and k' are fixed so that the average value of the combined potential vanishes. Defining this average difference as

$$\int_{C_1} (\Phi_2+\Phi_3)dy = 0$$

one has

$$kQ + \int_{C_1} k'\varphi_3 \cos(z,n)ds = kQ + k' \int_{C_1} \varphi_3 \frac{\partial\varphi_3}{\partial n} ds = 0$$

or

$$kQ = k'A_{B,\infty} \tag{17}$$

Equation (17) furnishes a companion relation to equation (16).

Kelvin's theorem gives

$$\iint\left[\left(\frac{\partial\Phi_1}{\partial y}\right)^2+\left(\frac{\partial\Phi_1}{\partial z}\right)^2\right]dy\,dz \leqq \iint\left[\left(\frac{\partial\Phi}{\partial y}\right)^2+\left(\frac{\partial\Phi}{\partial z}\right)^2\right]dy\,dz$$

where the integration extends over all two-dimensional space and the right-hand member evaluates the contribution of χ, Φ_2, and Φ_3. By means of Green's theorem, one has

$$(\sigma U_\infty-k)^2 \int \varphi_1 \frac{\partial\varphi_1}{\partial n} ds \geqq \int\left(\Phi_3 \frac{\partial\Phi_3}{\partial n} + \chi \frac{\partial\chi}{\partial n} + \Phi_2 \frac{\partial\Phi_2}{\partial n} + \chi \frac{\partial\Phi_2}{\partial n} + \Phi_2 \frac{\partial\chi}{\partial n}\right)ds$$

Since Φ_2 and χ are harmonic functions, the final two terms in the right integrand are equal. The inequality thus becomes

$$(\sigma U_\infty-k)^2 A_{W,\infty} \leqq k'^2 A_{B,\infty} + \sigma^2 U_\infty^2 A_{W,B} + k^2 Q - 2k\sigma U_\infty A_{W,B}$$

where $A_{W,B}$ is the apparent area of the wing-boundary region with the potential $\chi(y,z)$. Rearrangement of terms yields

$$\frac{(\sigma U_\infty-k)^2 A_{W,\infty}^2}{A_{W,\infty}} \leqq \frac{k'^2(A_{B,\infty}+Q)^2}{A_{B,\infty}+Q} + \frac{(k^2-k'^2)Q^2}{Q} + [(\sigma U_\infty-k)^2-k^2]A_{W,B}$$

If one divides by $(\sigma U_\infty-k)^2 A_{W,\infty} A_{W,B}$ and uses equations (16) and (17), the result is

$$\frac{1}{A_{W,B}}\left[\left(\frac{1}{Q}-\frac{1}{A_{B,\infty}+Q}\right)-\frac{1}{A_{W,\infty}}\right]\geqq\left[\left(\frac{1}{Q}-\frac{1}{A_{B,\infty}+Q}\right)^2-\left(\frac{1}{A_{W,\infty}}\right)^2\right]$$

The sign of the bracketed term on the left cannot be established in general but, if the inequality supplied by the minimum energy principle is used merely as an approximation formula, the relation can be simplified to give

$$\frac{1}{A_{W,B}}\approx\frac{1}{Q}-\frac{1}{A_{B,\infty}+Q}+\frac{1}{A_{W,\infty}} \tag{18}$$

Since from equation (15) minimum drag is

$$D=\frac{\sigma}{2}L=\frac{\rho_\infty}{2}U_\infty{}^2\sigma^2A_{W,B}$$

one has

$$D=\frac{L^2}{4q_\infty A_{W,B}}\approx\frac{L^2}{4q_\infty}\left(\frac{1}{Q}-\frac{1}{A_{B,\infty}+Q}+\frac{1}{A_{W,\infty}}\right) \tag{19}$$

R. T. Jones (ref. 8) has shown that the equality sign holds in this relation when the curve C_1 is an ellipse and the trace of the wing extends between the foci of C_1, a situation that always applies when the plan form of the wing is an ellipse. Further tests of the usefulness of equation (19) will be given in later sections.

APPLICATIONS

In this division some particular applications of the methods discussed above will be given. The first example, the elliptic wing, serves to illustrate a difficulty that can arise in the control-surface method for calculating drag. Next, some analog results are given, and, then, a family of wings with supersonic leading edges, having some interesting limiting forms, is treated. The concluding section shows how loading, integrated along oblique cutting lines, can be determined from general integral relations that apply to supersonic flow fields.

The Elliptic Wing of Given Volume

A wing of elliptic plan form leads to a boundary curve C_1 that is also an ellipse. Sketch (f) shows the wing, the boundary curves C_1 and C_2, and region S. Let C_1 be given by

$$\frac{y^2}{B^2} + \frac{z^2}{C^2} = 1$$

The solution of the problem where minimum drag with given volume is sought is eased by the fact that by manipulation of equation (6b), using the first of equations (12a), the expression for volume can be put in the form

$$V = -\frac{\beta^2}{U_\infty}\iint_S\left(\chi + \frac{\mu}{2\rho_\infty U_\infty} f^2\right) dy\, dz \qquad (20)$$

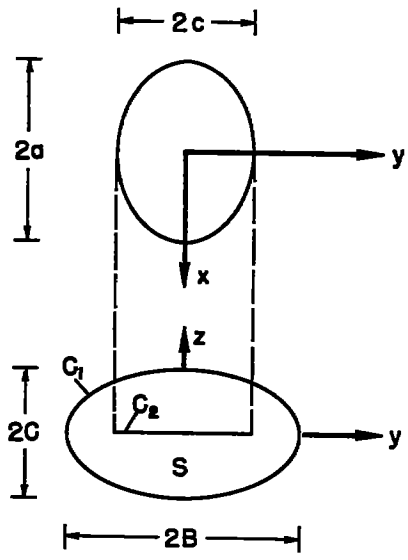

Sketch (f)

Thus, the explicit determination of χ from equations (12a) is avoided, and the complicated expression for f need never be used - only the fact that it vanishes on the outer boundary C_1. It is found that

$$\chi + \frac{\mu}{2\rho_\infty U_\infty} f^2 = -\frac{\mu}{2\rho_\infty U_\infty}\frac{\beta^2 B^2 C^2}{B^2+C^2}\left(\frac{y^2}{B^2} + \frac{z^2}{C^2} - 1\right) \qquad (21)$$

satisfies equations (12a). Substitution in equation (20) yields

$$V = -\frac{\mu}{8q_\infty}\beta^4\frac{B^2C^2S}{B^2+C^2}$$

where S is the area enclosed by C_1; $S = \pi BC$. Now, with the aid of equation (12b), the drag can be evaluated:

$$\frac{D}{q_\infty} = \frac{4V^2}{\beta^4 S}\left(\frac{1}{B^2} + \frac{1}{C^2}\right) \qquad (22a)$$

Finally, in terms of the original wing parameters a,c (see sketch (f))

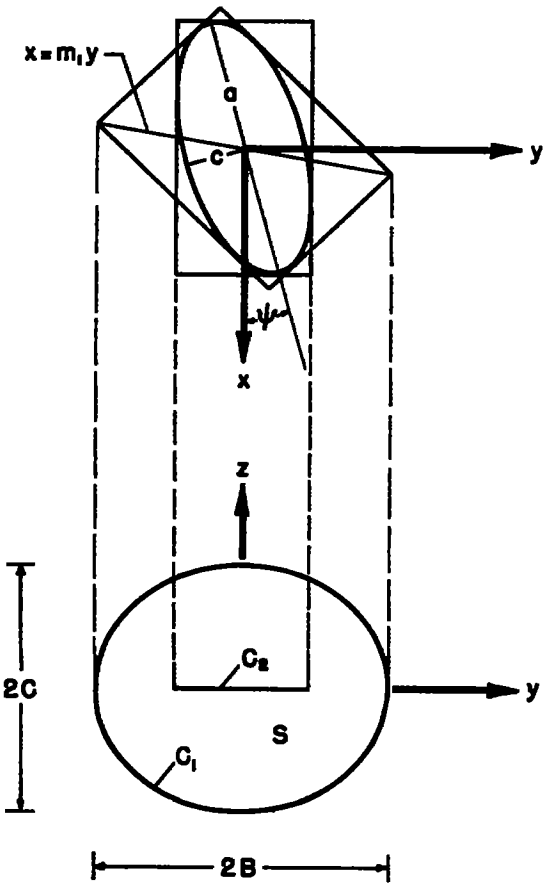

Sketch (g)

$$B^2 = a^2 + c^2/\beta^2$$

$$C^2 = c^2/\beta^2$$

$$\frac{D}{q_\infty} = \frac{4V^2}{(\pi ac)c^2}\,\frac{\beta^2+2\,\frac{c^2}{a^2}}{(\beta^2+c^2/a^2)^{3/2}} \tag{22b}$$

which agrees with the result of Jones in reference 9.

Next suppose that the elliptic wing is yawed. Then, as shown, in reference 3, the bounding curve Γ_1 lies in a plane $x = m_1 y$. Equations (12a) can be solved by the same device as used just above in the unyawed case, and the result is

$$\frac{D}{q_\infty} = \frac{8V^2}{\pi BC}\,\frac{1}{\beta^4}\,\frac{\frac{1}{B^2}+\frac{1}{C^2}}{2+\frac{m_1{}^2}{\beta^2}\left(3+\frac{B^2}{C^2}\right)} \tag{23}$$

which reduces properly to equation (22a) when $m_1 = 0$. In this case, the expressions for m_1, B, C in terms of the wing parameters a,c and the yaw angle ψ (see sketch (g)) are, if the wing eccentricity is $e^2 = 1-c^2/a^2$

$$\left.\begin{aligned}
m_1 &= (e^2\sin 2\psi)^{-1}\left[T-(T^2-\beta^2e^4\sin^2 2\psi)^{1/2}\right]\\
B^2/a^2 &= (2\beta^2)^{-1}\left[T+(T^2-\beta^2e^4\sin^2 2\psi)^{1/2}\right]\\
C^2/a^2 &= B^2/a^2 - (1-e^2\cos^2\psi)
\end{aligned}\right\} \tag{24}$$

where

$$T = \beta^2(1-e^2\cos^2\psi) + (1-e^2\sin^2\psi)$$

In this solution, the additional constraint of zero base area is enforced, as it was in the unyawed case (eq. (22b)) where the result checks that of Jones. The latter result applies to an elliptic wing that has zero base area, and, in fact, is closed all along the trailing edge, being of biconvex section. Jones also deduced, from considerations based on Hayes' principle of equivalent source position and the resultant evaluation of wave drag, that the optimum yawed elliptic wing has a biconvex section. Let the wing in unyawed position have upper and lower surfaces given by

$$z = \pm \frac{t}{2}\left(1 - \frac{x^2}{a^2} - \frac{y^2}{c^2}\right)$$

where t is the maximum thickness. The volume of this wing is

$$V = \frac{\pi}{2} tac$$

If this wing is yawed through an angle ψ (see sketch (g)), its drag can be found by a single integration (ref. 10):

$$\frac{D}{q_\infty} = t^2a^2c^2 \int_0^{2\pi} \frac{d\theta}{\mathbf{L}^4(\theta,\psi)} \tag{25}$$

with $m = \tan \psi$ and

$$\mathbf{L}^2(\theta,\psi) = \frac{1}{1+m^2}\left[(a^2+m^2c^2)-2\beta m(a^2-c^2)\cos\theta+\beta^2(m^2a^2+c^2)\cos^2\theta\right]$$

For the present purpose, it will be sufficient to consider the case where the minor axis $2c$ is small relative to the major axis $2a$. Then

$$\frac{D}{q_\infty} \approx \frac{8V^2}{\pi^2a^4}(1+m^2)^2\int_0^{\pi}\frac{d\theta}{(1-m\beta\cos\theta)^4} = \frac{4V^2}{\pi a^4}(1+m^2)^2\frac{2+3m^2\beta^2}{(1-m^2\beta^2)^{7/2}} \tag{26}$$

and this formula holds for $m\beta < 1$. For $m\beta > 1$, or when the wing is yawed outside the Mach cone, the drag is infinite. Equation (26) shows that the drag curve has a strong singularity as $m\beta \rightarrow 1$.

Now consider the limiting form of the drag given by equation (23) as $e^2 \rightarrow 1$, or $c/a \rightarrow 0$. It is

$$\frac{D}{q_\infty} \approx \frac{4V^2}{\pi a^4}\frac{2(1+m^2)^2(2-m^2\beta^2)}{(2+2m^2\beta^2-3m^4\beta^4)(1-m^2\beta^2)^{1/2}} \tag{27}$$

Comparison of this result with that of equation (26) shows the latter to be the greater except at $m = 0$ where they are equal. Thus, two minimum drags have been found, ostensibly for the identical constraints, and one is larger than the other. Thus it can be concluded that the larger drag results from a stricter constraint. This is certainly the case since pointwise trailing-edge closure is indeed more restrictive than zero base area, for the latter condition can be met by wings whose upper and lower surfaces cross to give an area distribution of changing sign at the trailing edge.

The present method for minimum drag calculation has thus led to a difficulty. The closure of a trailing edge is not an easy condition to express in terms of the control-surface integrals, so it does not seem feasible to force point-by-point closure by added constraints of the sort available. The element of uncertainty introduced by this situation, as to whether a determined minimum is achievable with a real wing, is certainly undesirable. However, the question only arises in nonlifting cases, since a negative ordinate on a cambered surface causes no unreality.

Analogous Variational Problems

In the previous section entitled "Solutions of Variational Problems" were listed the differential equations and boundary conditions that are satisfied by the optimizing potential $\chi(y,z)$ on the rear enveloping surface Σ_2 (see sketch (a)). If attention is limited to wings with supersonic leading edges, and the lift-area and moment-volume problems are considered in pairs, a similarity that shows up can be exploited. By virtue of the supersonic leading edges, the variational problems can be analyzed in the upper half-plane $z \geqq 0$, remembering, of course, that the flow and wing have vertical symmetry in the thickness case and that the flow field is antisymmetric in the lifting case. Consider, now, equations (11a) and (13a). The curve C_2 will be a portion of the axis $z = 0$ and the two problems will yield the same χ for $z \geqq 0$, and hence the same minimum drag if

$$\nabla^2 f = 0 \qquad \text{and} \qquad \lambda f_z]_{z=0} = 2q_\infty\sigma \tag{28}$$

It is found that a straight supersonic trailing edge yields a rear enveloping surface obeying equations (28). Let the trailing edge have the equation

$$x-ky = a \; ; \qquad k < \beta$$

The Σ_2 surface is an inclined plane, and

$$f(y,z) = ky \pm (\beta^2-k^2)^{1/2} z + a$$

$$f_z]_{z=0} = \pm(\beta^2-k^2)^{1/2}$$

Equations (28) give

$$\lambda = \pm 2q_\infty(\beta^2-k^2)^{-1/2}\sigma$$

Since drag is a quadratic function of χ, and since, from equations (11b) and (13b), equal drag occurs if

$$\frac{\lambda}{2} A = \frac{\sigma}{2} L$$

it suffices merely to set

$$L = \pm 2q_\infty(\beta^2-k^2)^{-1/2} A \tag{29}$$

Thus, if the minimum drag of a supersonic-edged wing with a straight trailing edge parallel to $x = ky$ of given base area is known, then it is also the minimum drag of the same wing considered as a lifting wing with lift determined by equation (29).

In this case, one needs to establish agreement between the relations

$$\left.\begin{aligned} \mu(2\beta^2+f\,\nabla^2 f) &= 2q_\infty\tau(z\,\nabla^2 f+2f_z) \\ \mu(ff_z)_{z=0} &= 2q_\infty\tau(f+zf_z)_{z=0} \end{aligned}\right\} \tag{30}$$

Equations (30) are satisfied by the same wing as in the previous case, except that k must be zero; that is, the trailing edge is normal to the free stream. In such a case

$$\mu = \pm \frac{2q_\infty\tau}{\beta}$$

and

$$\mathbb{M} = \pm \frac{2q_\infty}{\beta} V \tag{31}$$

This equation gives the pitching moment (at zero lift) of an optimum wing having the same optimum drag as the same wing carrying volume V with zero base area. The wings have supersonic edges and a straight trailing edge normal to the free stream.

Results of this sort have previously been noted between optimum drag configurations in subsonic lifting line theory and optimum slender bodies whose wave drag is given by the von Kármán formula. A summary of such results can be found in reference 11.

A Family of Wings With Supersonic Edges

Consider the family of wings whose plan forms are all portions of the hyperbola asymptotic to Mach lines through the point $(-d,0,0)$. The equation of the leading edge is

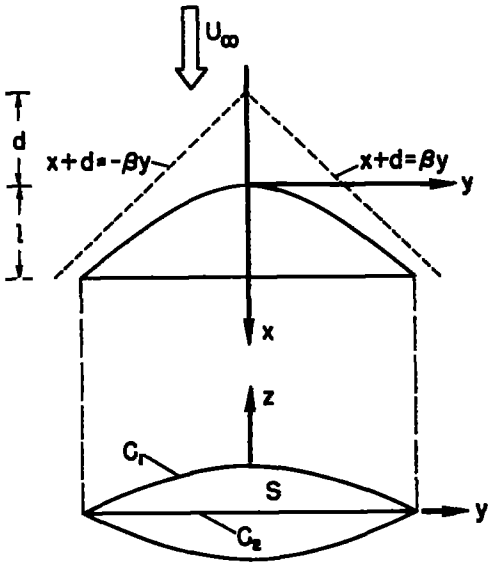

Sketch (h)

$$\beta^2 y^2 = 2dx + x^2$$

and the trailing edge is

$$x = l$$

where the quantities d and l are shown in sketch (h). The root chord of the resulting wing is l. If $d \to 0$, the wing becomes a triangle with sonic edges, and if $d/l \gg 1$, the wing has very large span compared with its chord.

The surface Σ_2 (sketch (a)) is composed of a pair of inclined planes

$$x = f(y,z) = l-\beta|z| \tag{32a}$$

and the boundary curve C_1 (sketch (h)) is made up of two parabolas

$$\beta^2 y^2 = (2d + l)(l-2\beta|z|) \tag{32b}$$

If minimum drag for fixed lift and center of pressure is sought for the wings of this family, the variation leads to the problem

$$\left.\begin{aligned} \nabla^2(\chi+U_\infty\tau zf) &= 0 \quad \text{in } S \\ \frac{\partial}{\partial n}\left[\chi+U_\infty(\sigma-x_m\tau)z+U_\infty\tau zf\right] &= 0 \quad \text{on } C_2 \\ \chi &= 0 \quad \text{on } C_1 \end{aligned}\right\} \tag{33}$$

where x_m is the coordinate of the center of pressure. A simple, exact solution of equations (33) follows directly if

$$x_m = d + \frac{3}{5} l$$

in which case

$$X = -\frac{3}{16} \frac{U_\infty \beta L}{[l(2d + l)]^{3/2}} \frac{z}{|z|} [\beta^2 y^2 + (2d + l)(2\beta|z| - l)] \tag{34}$$

In this event, the drag is given by

$$\frac{D}{q_\infty} = \frac{3}{4} \beta^2 \left(\frac{L}{q_\infty}\right)^2 \frac{d + \frac{3}{5} l}{[l(2d + l)]^{3/2}} \tag{35}$$

where L is the given lift. Since the wing area is

$$\frac{1}{\beta}\left[(d+l)\sqrt{l(2d + l)} - d^2 \cosh^{-1} \frac{d+l}{d}\right]$$

the drag parameter is, written in terms of $\zeta = d/l$

$$\frac{C_D}{\beta C_L^2} = \frac{9}{40} \frac{1 + \frac{5}{3}\zeta}{(1+2\zeta)^{3/2}} \left[(1+\zeta)\sqrt{1+2\zeta} - \zeta^2 \cosh^{-1}(1+\zeta)\right] \tag{36}$$

Sketch (i) shows the variation of the drag with ζ. This latter parameter is, in geometrical terms, $\beta^2 \rho_o / l$, where ρ_o is the radius of curvature of the leading edge at the apex, and l is root chord. As ζ varies from 0 to ∞, the plan form ranges from a sonic-edged triangle to a wing that has nearly a parabolic leading edge.

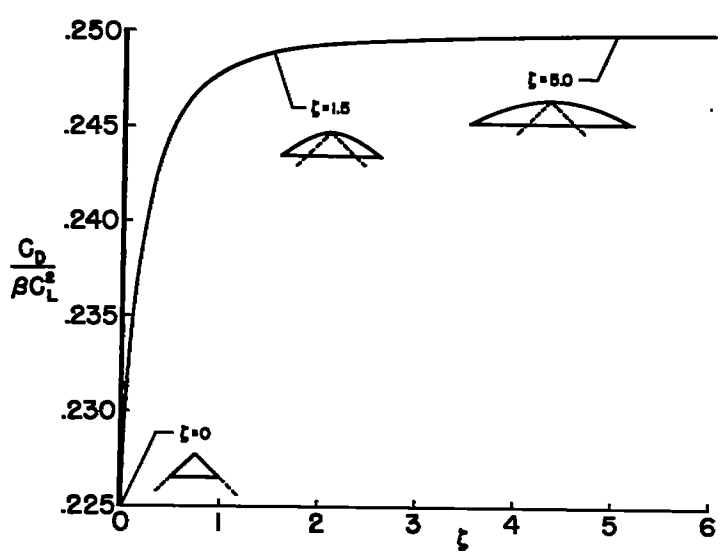

Sketch (i)

In the limit $\zeta \rightarrow 0$, when a sonic-edged triangular wing results, the value of the drag parameter given by equation (36) is

$$\frac{C_D}{\beta C_L^2} = 0.225 \tag{37}$$

This value is in agreement with the result of reference 4 for center of pressure at 60 percent of root chord. Also, the approximate result for given lift alone from reference 6 is quite close to that of equation (37), being 0.223. This would indicate that the center of pressure is near the 60-percent-chord position for given lift. In fact, from the results of reference 4, it is found that the center of pressure for given lift alone lies at 63 percent of the chord. The drag of the sonic-edged wing can also be calculated by the use of the approximation formula, equation (19). If the boundary C_1 is taken as an ellipse as a first crude approximation one gets

$$\frac{C_D}{\beta C_L^2} = 0.211$$

which differs from the result of reference 4 by about 5 percent.

At the other extreme, $\zeta \rightarrow \infty$, the wing plan form is very nearly a parabolic segment. The center of area of such a parabolic segment lies at 60 percent of the chord, which indicates that the loading is uniform over the wing. This is the correct result for minimum drag with given lift in two-dimensional flow, and the wing is indeed becoming nearly a two-dimensional case as $\zeta \rightarrow \infty$.

Triangular Wings With Subsonic Edges

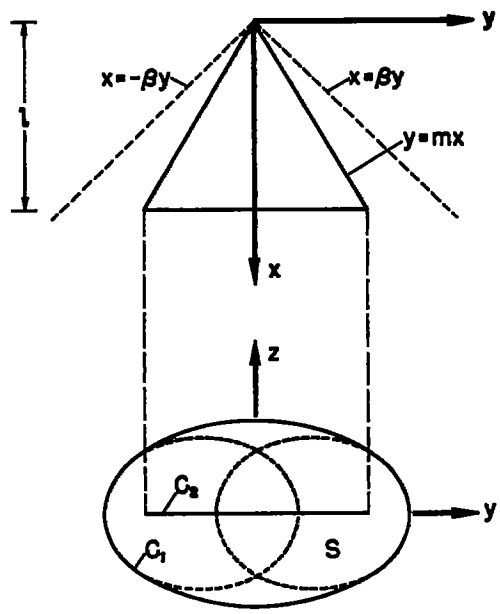

Sketch (j)

The approximation derived above as equation (19) can be used to predict drag of triangular wings with subsonic edges. The curve C_1 for such wings is shown in sketch (j). It is made up of a parabolic center section faired into ellipses. The equation to the upper parabola is

$$l^2 - 2\beta l z = \beta^2 y^2$$

and the ellipses are given by

$$\frac{(y \pm ml/2)^2}{(l/2\beta)^2} + \frac{z^2}{(1-m^2\beta^2)(l/2\beta)^2} = 1$$

The curve C_1 will be considered as an ellipse in order to find its apparent area;

$$A_{B,\infty} = (l/2\beta)^2 A^*_{B,\infty} = (l/2\beta)^2 \pi(1+m\beta)^2$$

The other necessary quantities are

$$A_{W,\infty} = (l/2\beta)^2 A^*_{W,\infty} = (l/2\beta)^2 4\pi m^2\beta^2$$

$$Q = (l/2\beta)^2 Q^*$$

$$= (l/2\beta)^2 \left[2\sqrt{1-m^2\beta^2}\cos^{-1}m\beta + \frac{2}{3}m\beta(9-m^2\beta^2)\right]$$

Then, from equation (19),

$$\frac{C_D}{\beta C_L^2} = m\beta\left(\frac{1}{Q^*} - \frac{1}{Q^*+A^*_{B,\infty}} + \frac{1}{A^*_{W,\infty}}\right) \tag{38}$$

The results of equation (38) are shown plotted in sketch (k). Also shown is the drag curve for a flat-plate wing. When $m\beta \rightarrow 0$ the predicted minimum is exact to the order of linear theory; when $m\beta \rightarrow 1$ the approximations used introduce an unconservative error, as was found in the last section in connection with the sonic-edged wing.

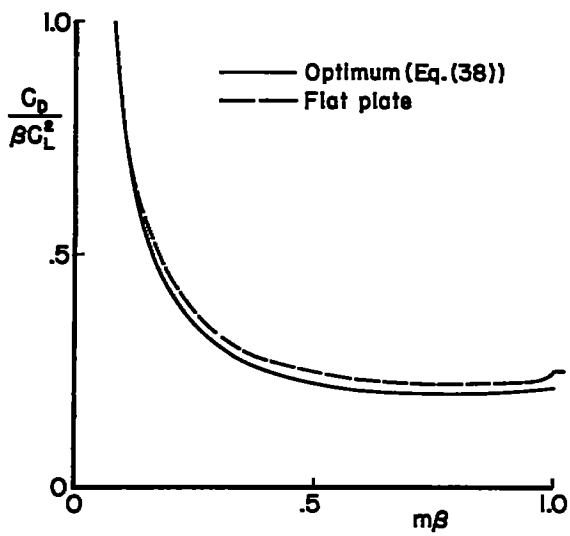

Sketch (k)

Integral Relations for Loading

The solution of the minimum drag problem provides a knowledge of the perturbation potential over the rear Mach surface Σ_2; the value of the perturbation potential at the trailing edge is therefore known and the spanwise load distribution follows directly. In the family of plan forms with hyperbolic leading edges, for example, equation (34) yields

$$\chi(y,0) = -\frac{3}{16}\frac{U_\infty \beta L}{[l(2d+l)]^{3/2}}[\beta^2 y^2 - l(2d+l)] \tag{39}$$

and the span loading remains parabolic for all members of the family.

It is also possible to relate the chordwise distribution of load to information supplied by $\chi(y,z)$, and the following development will derive results of this nature. The first objective will be to determine the magnitude of the load distribution integrated along an oblique line that lies in the plane of the wing. The line may be assumed to pass through the point $(x_o,0,0)$ and is to be inclined always at such an angle that the component of the free-stream velocity vector normal to it is supersonic; it thus lies in the so-called supersonic zone of silence that extends laterally from the point $(x_o,0,0)$. The method to be used is general in nature but, to avoid complication, attention will be directed principally toward the particular family of wings treated previously.

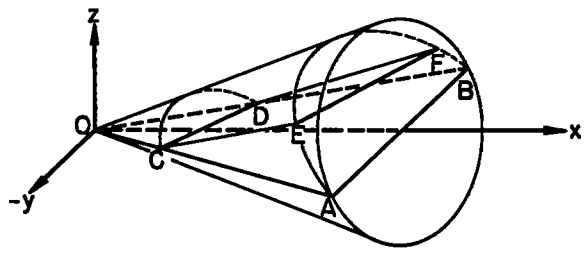

Sketch (l)

In sketch (l) let OAB represent a supersonic-edged plan form (not necessarily a triangle) and let the trailing edge AB be normal to the x axis. The cutting line CD is denoted

$$x - y \tan \mu_o = x_o \tag{40}$$

where μ_o is the angle between the line and the y axis and $\tan \mu_o \leqq \beta$. Two regions of interest need to be distinguished. The first (Region I), which corresponds to the geometry shown in the sketch, corresponds to the range of μ_o and x_o for which the cutting line does not intersect the trailing edge. The second (Region II) arises when an intersection with the trailing edge does occur within the confines of the plan form.

Region I.- Through the line CD pass two planes that are tangent to the double Mach cone with vertex at $(x_o,0,0)$. The forward and rearward inclined planes are, respectively, Σ_3 and Σ_4 and are represented by the linear equations

$$x - y\beta \cos \theta + z\beta \sin \theta = x_o \tag{41a}$$

$$x - y\beta \cos \theta - z\beta \sin \theta = x_o \tag{41b}$$

where

$$\tan \mu_o = \beta \cos \theta$$

The notation used in equations (41) is a common one in supersonic aerodynamics and was introduced first by W. D. Hayes in his treatment of equivalent source and doublet distributions (ref. 13).

If Green's theorem for equation (1) is applied to an arbitrary region enclosed by a continuous surface Σ, the fundamental integral relation

$$\iint_{\Sigma} \Lambda_o \frac{\partial\varphi}{\partial\nu} d\Sigma = 0 \tag{42}$$

results. The derivative $\partial\varphi/\partial\nu$ is the gradient of potential along the conormal ν with direction cosines ν_1, ν_2, ν_3 that are related to the direction cosines n_1, n_2, n_3 of the inner normal to the surface Σ by means of the relations

$$-n_1\beta^2 = \Lambda_o\nu_1 , \qquad n_2 = \Lambda_o\nu_2 , \qquad n_3 = \Lambda_o\nu_3 \tag{43}$$

Consider now the region enclosed by the surfaces Σ_1, Σ_2, Σ_3, and Σ_4. Each can be generated as the envelope of a family of Mach cones. In every case, therefore, $\Lambda_o = \beta$, the conormals lie along the surface, and the element of area can be expressed as $d\Sigma = d\nu\, ds$ where the element of arc ds is normal to $d\nu$ and lies on the surface. Locally, the surfaces are cones and the orthogonal curves to the conormals lie always in an x = const. plane. The line CD may be written

$$\left.\begin{aligned} x &= x_o+\beta y \cos\theta \\ z &= 0 \end{aligned}\right\} \tag{44}$$

and the line EF is

$$\left.\begin{aligned} x &= (l \sin\theta+x_o+\beta y \cos\theta)/(1+\sin\theta) \\ z &= (l-x_o-\beta y \cos\theta)/\beta(1+\sin\theta) \end{aligned}\right\} \tag{45}$$

An integration with respect to ν in equation (45) then gives, after noting that $\varphi = 0$ on Σ_4,

$$\frac{2}{\sin\theta}\int_C^D \varphi(x_o+\beta y \cos\theta, y, 0)dy$$

$$= \frac{1+\sin\theta}{\sin\theta}\int_E^F \varphi\left[\frac{l \sin\theta+x_o+\beta y \cos\theta}{1+\sin\theta}, y, \frac{l-x_o-\beta y \cos\theta}{\beta(1+\sin\theta)}\right] dy$$

If this equation is differentiated with respect to x_o, the desired integral relation is obtained

$$\int_C^D u(x_o+\beta y \cos\theta, y, 0)dy = -\frac{1}{2\beta}\int_E^F X_z(y,z)dy \tag{46}$$

In linearized theory, the local aerodynamic loading on a wing is given by $\Delta p/q_\infty = 4u_{(z=0+)}/U_\infty$. If the integrated loading along the line CD of equation (40) is denoted by $L(x_o,\theta)/q_\infty$, equation (46) assumes the convenient form

$$\frac{L(x_o,\theta)}{q_\infty} = -\frac{2}{\beta U_\infty}\int_E^F X_z dy \tag{47}$$

Region II.- The cutting line now intersects the trailing edge. Equations (41) again represent the forward and rearward inclined planes through CD and these planes intersect the surface Σ_2 along two lines. Sketch (m) indicates the geometry and shows, above, the plane $z = 0$ and, below, the projection of the figure as viewed in the direction of the negative x axis.

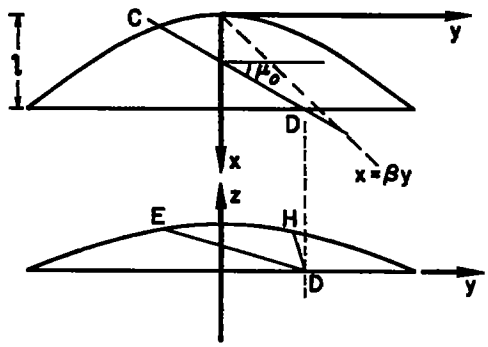

Sketch (m)

Equation (42) is again applied to the region enclosed by the surfaces Σ_1, Σ_2, Σ_3, and Σ_4, integration with respect to ν is carried out and followed by differentiation with respect to x_o. The analogous relations to equations (46) and (47) then appear in the form

$$\int_C^D u(x_o+\beta y \cos\theta, y, 0)dy = -\frac{1}{2\beta}\int_E^D X_z dy + \frac{1}{2\beta}\int_D^H X_z dy \tag{48}$$

$$\frac{L(x_o,\theta)}{q_\infty} = -\frac{2}{\beta U_\infty}\int_E^D X_z dy + \frac{2}{\beta U_\infty}\int_D^H X_z dy \tag{49}$$

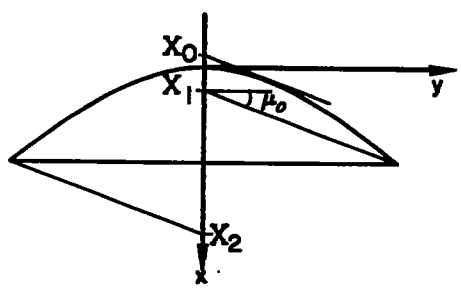

Sketch (n)

The above results can now be applied directly to the particular family of plan forms considered previously. For a fixed cutting angle μ_o, the range of x_o in Regions I and II is as shown in sketch (n). The values X_o, X_1, and X_2 are fixed, respectively, by the intersection of the wing's axis of symmetry and three parallel cutting lines. The first of these lines

is tangent to the leading edge of the plan form and the other two pass through the intersection points of the leading and trailing edges. One has $X_0 = -d(1-\sin\theta)$, $X_1 = l-(l^2+2ld)^{1/2}\cos\theta$, $X_2 = l+(l^2+2ld)^{1/2}\cos\theta$, and the following definitions

$$\text{Region I:} \quad X_0 \leqq x_0 \leqq X_1$$

$$\text{Region II:} \quad X_1 \leqq x_0 \leqq X_2$$

When $X_0 \geqq X_1$, Region I ceases to exist and this occurs when the angle μ_0 satisfies the inequality

$$\tan\mu_0 > \frac{\beta(l^2+2dl)^{1/2}}{l+d}$$

From equation (34),

$$\frac{1}{U_\infty}\chi_z = -\frac{3\beta^2}{8}\frac{L}{q_\infty}\frac{1}{l^{3/2}(l+2d)^{1/2}}$$

and the integration of equations (47) and (49) is immediate once the intersection points D, E, F, and H are calculated. These points are:

$$\text{D:} \quad y = (l-x_0)/\beta\cos\theta$$

$$\text{E:} \quad y = \frac{(l+2d)\cos\theta - \left\{2(l+2d)(1+\sin\theta)[x_0+d(1-\sin\theta)]\right\}^{1/2}}{\beta(1+\sin\theta)}$$

$$\text{F:} \quad y = \frac{(l+2d)\cos\theta + \left\{2(l+2d)(1+\sin\theta)[x_0+d(1-\sin\theta)]\right\}^{1/2}}{\beta(1+\sin\theta)}$$

$$\text{H:} \quad y = \frac{(l+2d)\cos\theta - \left\{2(l+2d)(1-\sin\theta)[x_0+d(1+\sin\theta)]\right\}^{1/2}}{\beta(1-\sin\theta)}$$

The integrated loadings become, finally,

<u>Region I</u>:

$$\frac{L(x_0,\theta)}{q_\infty} = \frac{3}{\sqrt{2}}\frac{L}{q_\infty}\frac{[x_0+d(1-\sin\theta)]^{1/2}}{l^{3/2}(1+\sin\theta)^{1/2}} \tag{50a}$$

Region II:

$$\frac{L(x_o,\theta)}{q_\infty}$$

$$= \frac{3}{\sqrt{2}}\frac{L}{q_\infty}\frac{1}{l^{3/2}}\left\{\frac{-(x_o+2d)}{[2(l+2d)]^{1/2}\cos\theta}+\frac{[x_o+d(1-\sin\theta)]^{1/2}}{2(1+\sin\theta)^{1/2}}+\frac{[x_o+d(1+\sin\theta)]^{1/2}}{2(1-\sin\theta)^{1/2}}\right\} \tag{50b}$$

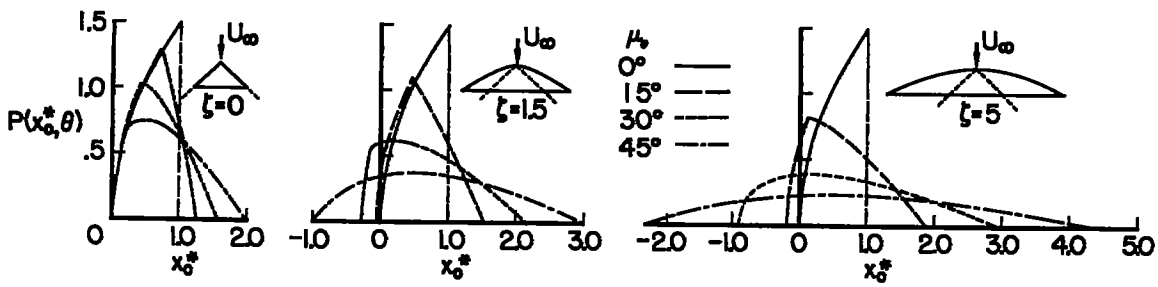

Sketch (o)

In sketch (o), these loadings are drawn for the three members of the family corresponding to $\zeta = d/l = 0, 1.5, 5$, with $\beta = 1$ and $\mu_o = 0^\circ$, 15°, 30°, 45° in each case. The dimensionless quantities plotted are

$$P(x_o^*,\mu) = \frac{L(x_o,\theta)}{q_\infty l}\cdot\frac{q_\infty l^2}{L}\ ; \qquad x_o^* = \frac{x_o}{l}$$

It is to be observed that when $\mu = 0$, $\theta = \pi/2$ and Region II ceases to exist. In this case the integrated loading is precisely the chord load distribution of the wing. One then gets the parabolic distribution

$$\frac{L(x_o,\pi/2)}{q_\infty} = \frac{3L}{2lq_\infty}\left(\frac{x_o}{l}\right)^{1/2}$$

For all other cutting angles the load distribution falls to zero at the two end points. In the case of the triangular plan form (d=0), the streamwise gradient of $L(x_o,\theta)$ has a square-root singularity at $x_o = 0$ for all cutting angles. This, in turn, requires a square-root singularity in the slope of the wing at $x_o = 0$.

Another integral relation between the loading and geometry of supersonic-edged wings can be found. If equation (42) is applied to the wing surface, the forward Mach surface, and the plane given by equation (41a), one finds, for Region I,

$$\int_C^D w(x_o+\beta y_1 \cos\theta, y_1)dy_1 = \beta \int_C^D u(x_o+\beta y_1 \cos\theta, y_1)dy_1 \tag{51}$$

and a similar result can be derived for Region II. Equation (51) can also be written

$$\frac{L(x_o,\theta)}{q_\infty} = \frac{4}{\beta U_\infty}\int_C^D w(x_o+\beta y_1 \cos\theta, y_1)dy_1 \tag{52}$$

Thus the integrated loading across the wing is proportional to the average value of the wing slope along the same direction. This result is not confined to optimum wings but is of interest in connection with the problem of finding the surface shape to support the optimum load distribution.

Ames Aeronautical Laboratory
National Advisory Committee for Aeronautics
Moffett Field, Calif., Nov. 29, 1957

REFERENCES

1. Nikolsky, A. A.: On the Theory of Axially Symmetric Supersonic Flows and Flows with Axisymmetric Hodographs. IX Int. Cong. Appl. Mech., Brussels, Sept. 1956.

2. Ward, G. N.: On the Minimum Drag of Thin Lifting Bodies in Steady Supersonic Flows. British A.R.C. Rep. 18,711, FM 2459, Oct. 1, 1956.

3. Heaslet, Max. A.: The Minimization of Wave Drag for Wings and Bodies With Given Base Area or Volume. NACA TN 3289, 1957.

4. Germain, Paul: Sur le minimum de traînée d'une aile de forme en plan donnée. Compte Rendus, tome 244, no. 9, 25 Fevrier 1957, pp. 1135-1138.

5. Germain, Paul: Aile symétrique à portance nulle et de volume donné réalisant le minimum de traînée en écoulement supersonique. Compte Rendus, tome 244, no. 22, 27 Mai 1957, pp. 2691-2693.

6. Graham, M. E.: Examples of Calculation of Minimum Supersonic Drag Due to Lift by Solution of Two-Dimensional Potential Problem: Elliptical-Planform Wings and an Approximate Delta-Planform Wing. Rep. No. SM-22754, Douglas Aircraft Co., Mar. 1957.

7. Lamb, H.: Hydrodynamics. Sixth ed. Dover Pub., N.Y., 1945.

8. Jones, R. T.: Minimum Wave Drag for Arbitrary Arrangements of Wings and Bodies. NACA Rep. 1335, 1957. (Supersedes NACA TN 3530)

9. Jones, R. T.: Theoretical Determination of the Minimum Drag of Airfoils at Supersonic Speeds. Jour. Aero. Sci., vol. 19, no. 12, Dec. 1952.

10. Lomax, Harvard, and Heaslet, Max. A.: A Special Method for Finding Body Distortions That Reduce the Wave Drag of Wing and Body Combinations at Supersonic Speeds. NACA Rep. 1282, 1956.

11. Heaslet, Max. A., and Lomax, Harvard: Supersonic and Transonic Small Perturbation Theory. Sec. D of General Theory of High Speed Aerodynamics. Vol. VI of High Speed Aerodynamics and Jet Propulsion. W. R. Sears, ed., Princeton Univ. Press, 1954, pp. 122-344.

12. Graham, E. W.: The Calculation of Minimum Supersonic Drag by Solution of an Equivalent Two-Dimensional Potential Problem. Rep. No. SM-22666, Douglas Aircraft Co., Dec. 1956.

13. Hayes, Wallace D.: Linearized Supersonic Flow. Rep. No. AL-222, North American Aviation, Inc., June 18, 1947.

NACA - Langley Field, Va.